Journal of Biomechanics 82 (2019) 38–45

Contents lists available at ScienceDirect

Journal of Biomechanics

journal homepage: www.elsevier.com/locate/jbiomech
www.JBiomech.com

Measurement of local diffusion and composition in degraded articular cartilage reveals the unique role of surface structure in controlling macromolecular transport

Chris D. DiDomenico [a], Aydin Kaghazchi [a], Lawrence J. Bonassar [a,b,*]

[a] Meinig School of Biomedical Engineering, Cornell University, Ithaca, NY, United States
[b] Sibley School of Mechanical and Aerospace Engineering, Cornell University, Ithaca, NY, United States

ARTICLE INFO

Article history:
Accepted 17 October 2018

Keywords:
Proteoglycans
Collagenase
Arthritis
Antibody transport
Matrix degradation

ABSTRACT

Developing effective therapeutics for osteoarthritis (OA) necessitates that such molecules can reach and target chondrocytes within articular cartilage. However, predicting how well very large therapeutic molecules diffuse through cartilage is often difficult, and the relationship between local transport mechanics for these molecules and tissue heterogeneities in the tissue is still unclear. In this study, a 150 kDa antibody diffused through the articular surface of healthy and enzymatically degraded cartilage, which enabled the calculation of local diffusion mechanics in tissue with large compositional variations. Local cartilage composition and structure was quantified with Fourier transform infrared (FTIR) spectroscopy and second harmonic generation (SHG) imaging techniques. Overall, both local concentrations of aggrecan and collagen were correlated to local diffusivities for both healthy and surface-degraded samples ($0.3 > R^2 < 0.9$). However, samples that underwent surface degradation by collagenase exhibited stronger correlations ($R^2 > 0.75$) compared to healthy samples ($R^2 < 0.46$), suggesting that the highly aligned collagen at the surface of cartilage acts as a barrier to macromolecular transport.

1. Introduction

One of the most prominent types of joint disease is osteoarthritis (OA), for which a clear, effective treatment remains elusive. Recent research supports that chondrocytes within articular cartilage play a large role in joint disease initiation and progression by producing inflammatory cytokines such as interleukin-1 (IL-1) and tumor necrosis factor-alpha (TNF-α) (Evans et al., 2013; Gerwin et al., 2006; Martel-Pelletier, 2004; Moos et al., 1999; Shimizu and Ohta, 2015). The use of antibodies (150 kDa) to bind to and inhibit these factors has been very successful in treating other diseases, such as rheumatoid arthritis (RA) (Chan et al., 2009; Feldmann and Maini, 2001). However, there is concern that these drugs will have trouble diffusing through the avascular articular cartilage to target source cells *in vivo*, especially since synovial fluid clearance times are on the order of hours (Allen et al., 2010; Gerwin et al., 2006; Goldring, 2001; Martel-Pelletier, 2004; Moos et al., 1999). As such, macromolecular transport into the inherently complex cartilage tissue is an active area of investigation.

There are well-known depth-dependent variations in composition and structure within articular cartilage, which is composed of mainly of type-II collagen and aggrecan (Mow et al., 1984; Poole et al., 2001). Aggrecan, a large negatively charged proteoglycan, is responsible for a very small matrix pore size (Maroudas, 1975) and an increasing matrix density deeper in the tissue (Maroudas and Bullough, 1968; Mow et al., 1984; Poole et al., 2001). Near the surface, collagen fibers are dense and highly aligned, but fiber organization changes throughout the depth of the tissue (Hwang et al., 1992). The highly heterogeneous nature of this tissue has many implications for molecular diffusion. Several studies have shown that there are depth-dependent diffusive mechanics for a wide range of large solutes (DiDomenico et al., 2017; Leddy et al., 2006; Leddy and Guilak, 2003). However, these studies lack explicit correlations between local matrix composition and local diffusivity. Developing such relationships for larger therapeutics would be helpful in healthy tissue, but it is also important to consider how disease or degradation of cartilage affects these relationships.

Clinical progression of many types of arthritis manifests itself by losses in aggrecan and collagen density (Bank et al., 2000, 1997; Hwang et al., 1992; Martel-Pelletier et al., 1994; Sun, 2010; Treppo et al., 2000; Venn and Maroudas, 1977), which have

* Corresponding author at: Meinig School of Biomedical Engineering, 149 Weill Hall, Cornell University, Ithaca, NY 14853, United States.
E-mail address: lb244@cornell.edu (L.J. Bonassar).

https://doi.org/10.1016/j.jbiomech.2018.10.019
0021-9290/

important implications for bulk drug transport (Clark, 2001; Lotke and Granda, 1972; Torzilli et al., 1997). To mimic *in vivo* degradation, matrix metalloproteinase-1 (MMP-1) (Case et al., 1989; Nguyen et al., 1989; Pelletier et al., 1988) and other inflammatory cytokines, such as IL-1 (Chin et al., 1985; Pelletier et al., 1988) and TNF-α (Chin et al., 1985; MacNaul et al., 1990), have been used to investigate the effects of degradation on cartilage structure and solute diffusion mechanics. These studies have demonstrated decreases in bulk and local mechanical properties (Elliott et al., 2002; Griffin et al., 2014; Hayes and Bodine, 1978; Williamson et al., 2003; Wilson et al., 2004; Zhu et al., 1993) and increases to solute diffusion (Lotke and Granda, 1972; Torzilli et al., 1997). Specifically, Torzilli reported an inverse dependence of solute diffusivity on local aggrecan content for inulin and 70 kDa dextran molecules (Torzilli et al., 1997). Interestingly, diffusion of even larger molecules (e.g. antibodies, 150 kDa) exhibit unexpectedly slow diffusion through the superficial region (DiDomenico et al., 2017), which is relatively low in aggrecan content (Silverberg et al., 2014). As such, it is hypothesized that these molecules are heavily affected by collagen structure, but this relationship has not been fully elucidated.

Therefore, the overarching goal of this study is to investigate the relationship between local cartilage structure and composition and its effect on local antibody diffusion mechanics. Specifically, this study aims to elucidate the role of the surface layer of cartilage with regards to its effect on macromolecular diffusion through the articular surface.

2. Methods

2.1. Cartilage harvest, preparation, and cartilage surface degradation

As described previously (DiDomenico et al., 2017), fresh, sterile, 2 mm full-thickness cartilage was harvested from the patellofemoral groove of 1–3 day old bovine calves (~10 experiments/animals) (Gold Medal Packing, Rome, NY). These plugs (~16 per experiment) were rinsed in sterile phosphate buffered saline (PBS) (Corning, NY) and randomly assigned to two groups: undegraded (healthy) and surface-degraded (n = 8 per group). Surface-degraded samples had a drop (~10 μl) of either two different enzymes applied to the articular surface for 30 min at 37 °C (Fig. 1): 2 mg/mL of bacterial collagenase (Worthington, type II collagenase, Lakewood, NJ), to degrade both proteoglycans and collagen (Billinghurst, 1997; Griffin et al., 2014), or 200 μg/mL of trypsin (Cellgro, 0.25% trypsin EDTA, Manassas, VA), to degrade only proteoglycans (Griffin et al., 2014; Nguyen et al., 1989). Sufficient surface tension of the drop prevented accidental degradation of the sides of the cartilage plugs. After degradation, samples were serially rinsed with protease inhibitors in 1x PBS for 10 min.

2.2. Solute transport setup

For all samples, 2 × 4 × 1.15 mm slices of tissue were obtained (DiDomenico et al., 2017) and placed in two 24-well plates (one for healthy and one for degraded) such that the articular surface and deep zones were exposed to media on lateral faces (Fig. 1). To limit unwanted diffusion and tissue swelling (DiDomenico et al., 2017, 2016), an impermeable platen array was placed on top of each 24-well plate, compressing all samples ~15%. As in another study (DiDomenico et al., 2017), 350 μl of a chemically-stable (DiDomenico et al., 2017, 2016), fluorescently-labeled (Alexa Fluor 633) antibody (150 kDa) solution (gift from Andrew Goodearl and Anna Yarilina from AbbVie Inc, Worcester, MA) was added to each well at a concentration of ~2.5 μM in PBS. Samples were exposed to this solution for 3 h (DiDomenico et al., 2017, 2016).

2.3. Solute transport analysis (1-D spatial diffusion model)

After solute exposure, all slices were bisected perpendicular to the articular surface (DiDomenico et al., 2017). This cut surface of one of these slices (2 × 2 × 1.15 mm) was assessed on a confocal microscope stage (LSM 710, Zeiss, Germany) to characterize antibody penetration perpendicular to the articular surface (Fig. 1). Confocal microscope and laser settings were similar to those described previously (DiDomenico et al., 2017, 2016). Column-wise pixel averages of sample image data (hereby defined as fluorescence profiles) were obtained from the articular surface to 1000 μm deep into the tissue. The sample geometry, averaging technique, and cutting procedure in these experiments mitigated the effects of diffusion in directions that were not perpendicular to the articular surface and other imaging artifacts (DiDomenico et al., 2017, 2016). These fluorescence profiles were used in place of concentration profiles to inform local solute diffusion calculations (DiDomenico et al., 2017, 2016).

Fluorescence profiles (normalized to the fluorescence value at x = 0 μm) were broken down into discrete "layers," spaced 35 μm apart, for a total of 28 layers per sample (from 0 to 1000 μm). Using a root mean square (RMS) error minimization procedure for each layer, fluorescence data within that particular layer was fit to the appropriate local solution of a multi-layer, transient slab diffusion equation in 1D (Carr and Turner, 2015), as utilized in previous studies (DiDomenico et al., 2017, 2016). The transport model was used to calculate how solute diffusivity is affected locally throughout the depth in both healthy and degraded samples (Fig. 2). Model assumptions and boundary conditions were the same as previously described (DiDomenico et al., 2017, 2016).

2.4. Analysis of gross sample composition (Biochemistry)

Using the same bisected half of cartilage used for confocal imaging, biochemical analyses were performed, as previously described (Ballyns et al., 2008; Middendorf et al., 2017). These samples were weighed, refrozen, lyophilized, and weighed again. Samples were then digested with 1.25 mg/mL papain solution (Sigma-Aldrich, St. Louis, MO) overnight at 60 °C and analyzed for sulfated glycosaminoglycan (GAG) content through a 1,9-dimethylmethylene blue assay (Enobakhare et al., 1996) and for collagen through a hydroxyproline assay (Neuman and Logan, 1950). Biochemical properties were normalized to the dry weight of the samples and averaged within healthy and degraded groups.

2.5. Analysis of spatial aggrecan sample composition (Histology)

The other 2 × 2 × 1.15 mm section of cartilage was then fixed in formalin, embedded in paraffin, and sectioned into 4-μm thick sections on glass slides. Samples were dewaxed in serial xylene baths and rehydrated in serial washes of ethyl alcohol (Silverberg et al., 2014). These samples were then stained with Safranin-O for 11 min and dehydrated to visualize aggrecan within the tissue (Fig. 3).

2.6. Analysis of spatial aggrecan content (Fourier transform infrared spectroscopy)

As reported previously (Silverberg et al., 2014), 4-um thick sections of all samples were also placed on 2-mm-thick, 25 mm diameter infrared transparent BaF_2 disks (Spectral Systems, Hopewell Junction, NY). In transmission mode, a Hyperion 2000 Fourier transform infrared imaging (FTIR) microscope (Bruker, Billerica, MA) obtained sample absorbance spectra (average of 32 background-corrected scans between 600 and 4000 cm^{-1}) with a resolution of 4 cm^{-1} using a 15× objective (Silverberg et al.,

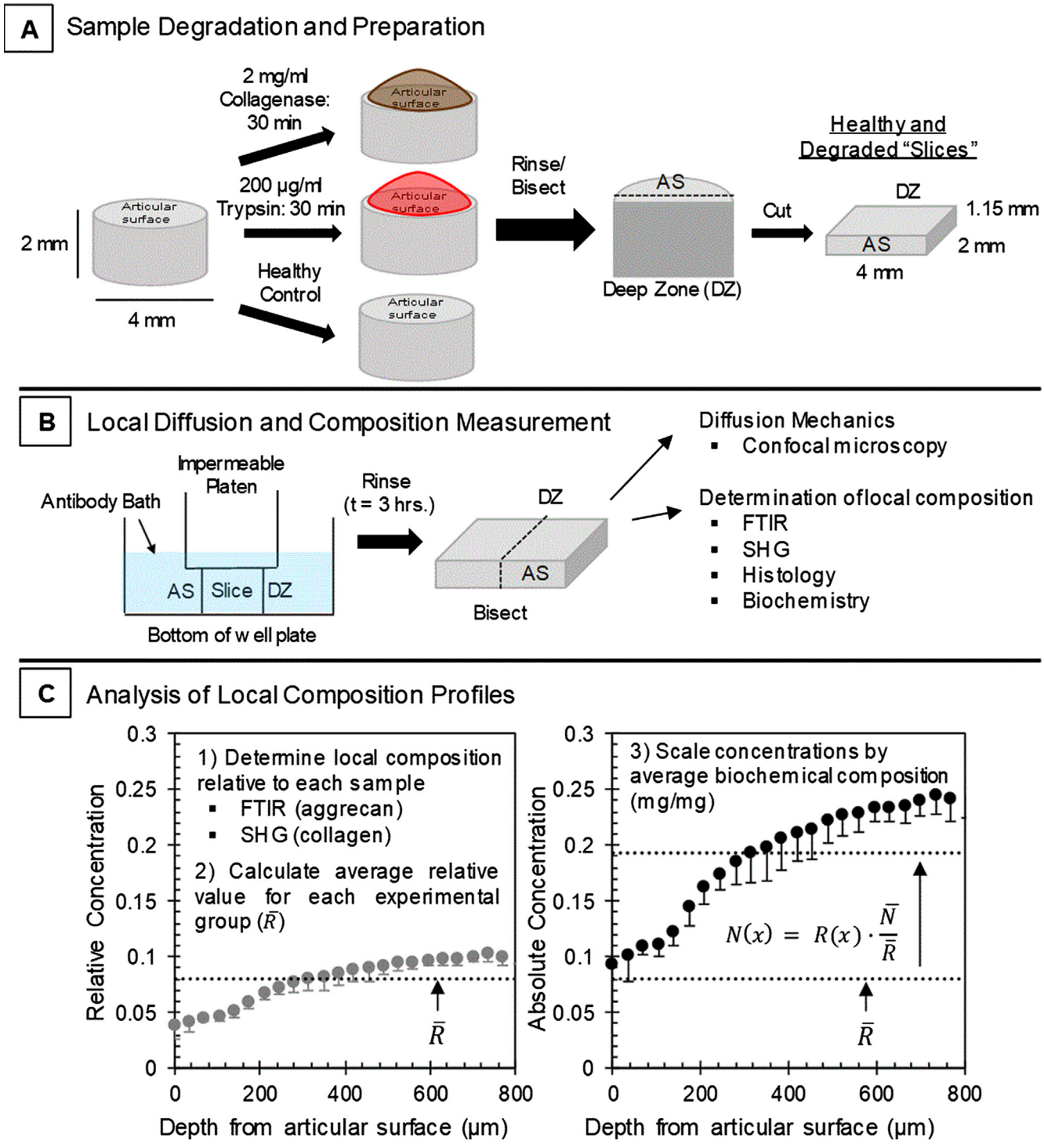

Fig. 1. During sample preparation (A), cartilage explants were randomly assigned to three groups: 2 mg/ml collagenase, 200 µg/ml trypsin, or healthy controls. With the bottom third of all samples submerged in PBS, drops (~10 µl) of collagenase or trypsin were added to the articular surface of samples. After rinsing with protease inhibitors, samples were cut to obtain slices measuring 4 × 2 × 1.15 mm. Degraded and healthy slices were then exposed to a fluorescent antibody solution (B) so that diffusion would occur perpendicularly to the articular surface. After 3 h of exposure, samples diffusion was examined with confocal microscopy. Compositional analysis was also performed with Fourier transform infrared spectroscopy (FTIR), second harmonic generation (SHG) imaging, biochemistry, and histology. Bulk aggrecan and collagen content were calculated with biochemistry techniques, and was normalized to dry weight for each group (N) (mg/mg). Using the average relative composition from FTIR and SHG ($\bar{R}$), relative concentrations were scaled point by point by the ratio of $\bar{N}$ and $\bar{R}$.

2014). These absorbance spectra were collected at equally spaced intervals (35 µm) over a rectangular region of 25 × 120 mm^2, from the articular surface to the deep zone. Using a previously validated method (Silverberg et al., 2014), spectra were fit to a linear combination of a pure type II collagen spectrum (Camacho et al., 2001), a pure aggrecan spectrum (Camacho et al., 2001), and a linear baseline over a spectral window from 900 to 1725 cm^{-1} (Silverberg et al., 2014). The resulting depth-wise, pure-compound aggrecan coefficient, which is proportional to molecular concentration (Silverberg et al., 2014), was scaled to the results of the

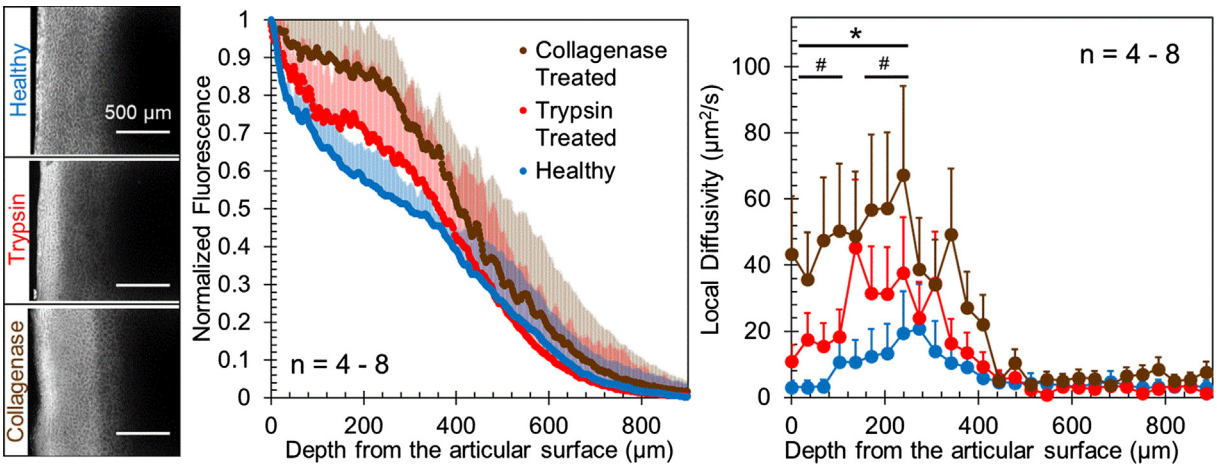

Fig. 2. Fluorescence images allow calculation of fluorescence profiles for all three groups and determination of how degradation affects local solute diffusivities (left). Transport analyses showing the fluorescence curves of all experimental conditions (middle) and their respective local diffusivities throughout the depth of the cartilage (right). Samples with the surfaces degraded by either enzyme (collagenase or trypsin) exhibited higher fluorescence compared to the healthy controls within the first 400 μm from the articular surface. Degradation with either trypsin or collagenase led to higher diffusivities compared to healthy within the first 350 μm (*: $p < 0.05$, repeated-measures two-way ANOVA), and all groups were statistically similar at depths >400 μm (with an average of 4 $\mu m^2/s$). Collagenase-treated samples exhibited the highest local diffusivities (70 $\mu m^2/s$ at 250 μm), compared to the trypsin-treated (40 $\mu m^2/s$ at 250 μm) or healthy samples (20 $\mu m^2/s$ at 250 μm), and highest diffusivities at the surface (0 μm) of the tissue (45 $\mu m^2/s$), compared to the trypsin (10 $\mu m^2/s$) or healthy (4 $\mu m^2/s$) groups ($p < 0.05$). Error bars (both shaded and standard) denote standard deviations with n = 4–8.

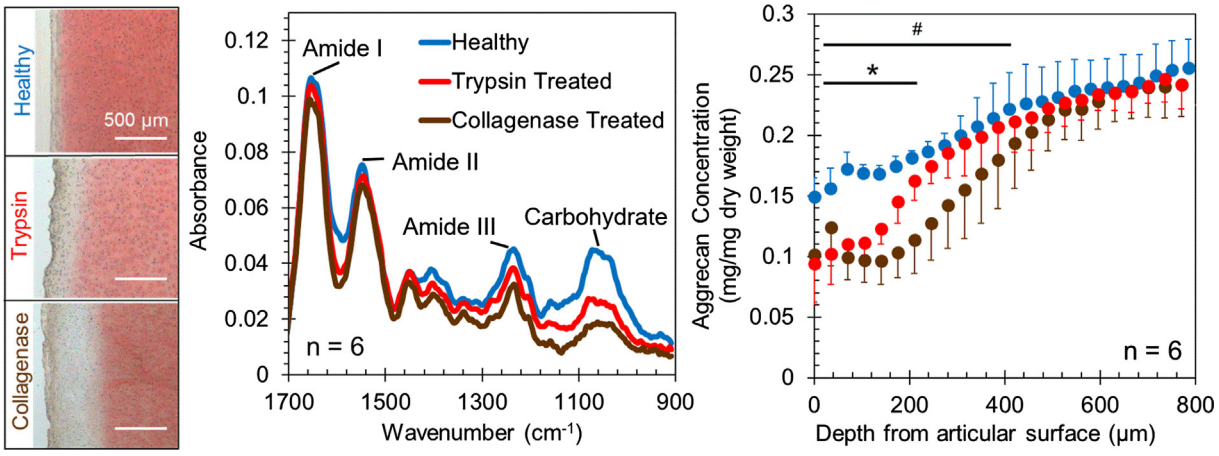

Fig. 3. Safranin-O histology images (left) demonstrate how trypsin and collagenase degrade the proteoglycans near the surface zone of the cartilage. Absorbance spectra from FTIR analysis for the degraded samples compared to normal healthy controls (middle) at a depth of 100 μm. Collagenase and trypsin both drastically changed the absorbance spectra by altering the carbohydrate peak height near (1140–985 cm^{-1}), suggesting collagenase caused greater loss of proteoglycans (including aggrecan) compared to trypsin. Local aggrecan composition (right) was obtained by calculating the depth-dependent aggrecan fitting coefficient by decomposing FTIR absorbance data (Silverberg et al., 2014). This coefficient was scaled to the average dry-weight aggrecan concentration obtained from biochemical analysis for each group (21–23%) (see Supplementary Fig. 1). Degradation with collagenase or trypsin led to significant decreases (up to 40%) in aggrecan content, within the first 210 and 420 μm, respectively ($p < 0.05$). Aggrecan content was statistically similar past 420 μm.

biochemical analysis of tissue samples by a single multiplicative factor. This factor was equal to the average group-specific aggrecan content from biochemistry (~ 22% of the dry weight) divided by the average pure-compound aggrecan coefficient for each sample (see Fig. 1). Using this factor enabled the calculation of absolute, group-specific, depth-wise concentrations of aggrecan (Fig. 3).

2.7. Analysis of spatial collagen content (second harmonic generation imaging)

Although the FTIR method enabled calculation of the spatial collagen content, this method could not quantify disruption of the organization of the collagen matrix in degraded samples. As such, second harmonic generation (SHG) imaging was used to obtain a better overall picture of how this degradation protocol affected the concentration of *organized* collagen through the depth of the tissue (Chen et al., 2012). Using the bisected sample halves used for histology, an upright confocal microscope capable of SHG imaging (LSM 880, Zeiss, Germany) was used to image 13-μm thick, deparaffinized sections of all samples. A 20× water-immersion objective with a numerical aperture of 0.17 captured a ~1.5 μm optical slice of each sample with a resolution of 0.35 μm/pixel. A circular polarizer was used to prevent changes in collagen orientation from affecting SHG intensity. With a laser excitation wavelength of 880 nm, a non-descanned detector (NDD) was used to capture SHG intensity profiles from the articular surface to the deep zone of the tissue (0–1000 μm) with a 430–455 nm wavelength filter in place to mitigate autofluorescence of the collagen and other matrix constituents. Column-wise pixel averages of SHG image data were then obtained and converted to organized

collagen concentration by taking the square root of each averaged pixel value (Chen et al., 2012). This depth-wise collagen concentration map for each sample was normalized to group-specific gross collagen content (~52% of the dry weight) obtained from biochemistry, which resulted in absolute, organized collagen concentrations for all samples (Fig. 4).

2.8. Statistical analysis

Repeated-measures two-way analysis of variance (ANOVA) was performed to determine the effect of degradation and depth (the repeated-measure) from the articular surface on local diffusivities and local composition, with subsequent Tukey post-hoc tests for pairwise comparisons. Linear regression was performed to assess the relationship between local diffusivities and composition. Analysis of covariance (ANCOVA) was used to compare relationships between diffusivity and composition. All statistics were carried out in Minitab 17 Statistical Software (State College, PA).

3. Results

3.1. Transport analysis

For healthy and degraded samples, the shape of the fluorescence profiles obtained from confocal images suggest that diffusion behavior is highly heterogeneous throughout the depth of the tissue, consistent with previous studies (DiDomenico et al., 2017, 2016; Leddy and Guilak, 2003). Degrading cartilage samples with collagenase or trypsin increased local fluorescence values up to 50% compared to healthy controls within 0–400 μm of the surface and changed the shape of the fluorescence profiles in this region, but no differences between groups were found beyond that depth. Increases in local fluorescence were observed in areas of lower aggrecan in all samples (Fig. 2), supporting the idea that aggrecan content and local transport mechanics are highly related.

Using a validated multi-layer diffusion model with layers spaced every ~35 μm (DiDomenico et al., 2017), all samples exhibited heterogeneous diffusivities through the depth of the tissue (Fig. 2). Healthy samples exhibited a maximum local diffusivity of 20 $\mu m^2/s$ at 250 μm from surface ($p < 0.05$, repeated-measures two-way ANOVA), whereas values near the articular surface (0–100 μm) and deeper zones (>400 μm) were about 4 $\mu m^2/s$ (Fig. 2). Degradation with either trypsin or collagenase led to higher diffusivities within the first 350 μm ($p < 0.05$), and all groups were statistically similar at depths >400 μm. Collagenase-treated samples exhibited the highest local diffusivities (70 $\mu m^2/s$ at 250 μm), compared to the trypsin-treated (40 $\mu m^2/s$ at 250 μm) or healthy samples, and highest diffusivities at the surface (0 μm) of the tissue (45 $\mu m^2/s$), compared to the trypsin (10 $\mu m^2/s$) or healthy (4 $\mu m^2/s$) groups ($p < 0.05$).

3.2. FTIR analysis (local aggrecan composition)

A previously established (Silverberg et al., 2014), linear decomposition analysis was conducted to analyze how aggrecan content varied as function of depth in cartilage. Linearly decomposed spectra closely fit the actual FTIR absorbance spectra at all tissue depths, with average errors between 10 and 15%. Overall, the biochemistry-scaled aggrecan composition of both healthy and degraded samples varies as a function of depth (Fig. 3), as previously reported (Silverberg et al., 2014). Degradation with collagenase or trypsin led to significant decreases (up to 40%) in aggrecan content, within the first 210 and 420 μm, respectively ($p < 0.05$) (Fig. 3). Consistently, there were visible decreases in Safranin-O histological staining intensity in the first 0–250 μm from the articular surface in samples that were treated with trypsin and collagenase. At 100 μm, the FTIR absorbance spectra for degraded samples exhibited lower absorbance values near wavenumbers (~1140–985 cm^{-1}) associated with carbohydrate content (Camacho et al., 2001; Khanarian et al., 2014; Saarakkala and Julkunen, 2010), consistent with these samples containing lower amounts of proteoglycan (aggrecan) near the surface. Absorbances near the amide I (1720–1590 cm^{-1}) and amide III (1590–1492 cm^{-1}) regions (Khanarian et al., 2014) were similar for all groups and depths, suggesting that that the gross amount of collagen content was unchanged across all sample groups.

3.3. SHG analysis (local collagen composition)

Because FTIR could not identify the effects of collagenase on collagen organization, SHG imaging was used to assess local composition of *organized* collagen, scaled to biochemistry data (Chen et al., 2012). Overall, organized collagen concentration for the healthy group mirrored compositional trends in collagen reported elsewhere (Khanarian et al., 2014; Silverberg et al., 2014). As anticipated, organized collagen concentrations in trypsin-treated samples did not differ significantly from healthy controls, but collagenase-treated samples exhibited significantly lower organized collagen concentrations within the first 50 μm from the articular surface ($p < 0.05$) (Fig. 4).

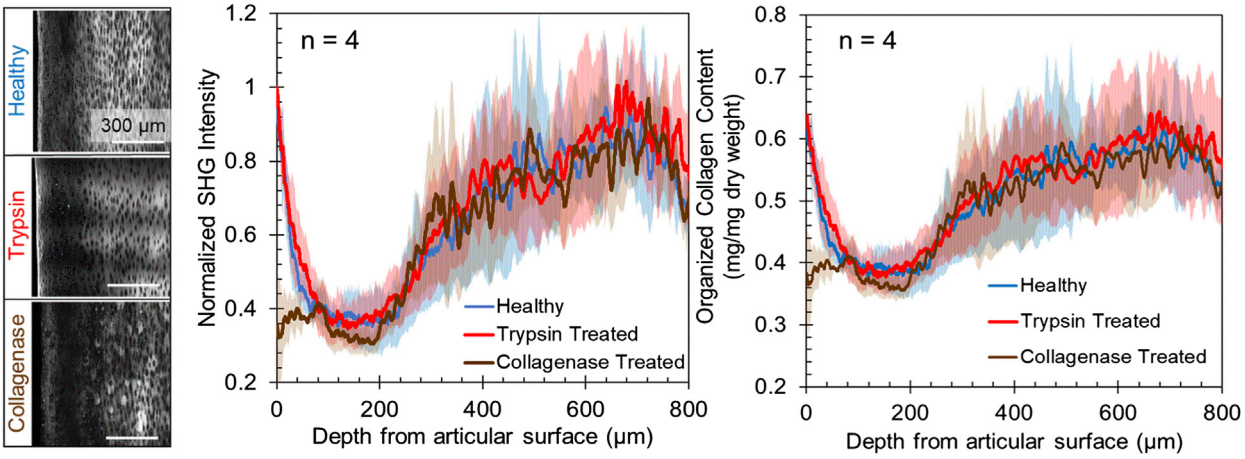

Fig. 4. SHG images demonstrate how these enzymes affect the distribution of organized collagen in the tissue (left) and normalized SHG intensity profiles (middle). As anticipated, organized collagen concentrations in trypsin-treated samples did not differ significantly from healthy controls (right), but collagenase-treated samples exhibited significantly lower organized collagen concentrations within the first 50 μm from the articular surface ($p < 0.05$).

3.4. Correlation analysis

Local diffusivities were compared to local collagen content obtained from SHG and local aggrecan content obtained from FTIR analyses. Overall, local diffusivity was negatively correlated with concentrations of collagen and aggrecan in all groups (Fig. 5). Additionally, aggrecan and collagen content were more strongly correlated with diffusivity in the degraded groups (trypsin: $R^2 = 0.45$, 0.74, $p < 0.001$; collagenase: $R^2 = 0.86$, 0.75, $p < 0.001$), compared to the healthy group ($R^2 = 0.31$, 0.46, $p < 0.01$). Furthermore, aggrecan and collagen correlations for collagenase-treated samples exhibited steeper diffusivity/concentration relationships compared to correlations from the healthy group ($p < 0.05$, ANCOVA).

4. Discussion

The goal of this study was to investigate how the spatial diffusion patterns of diffusion of an antibody relate to local cartilage structure and composition in healthy and degraded samples. Consistent with previous research (DiDomenico et al., 2017), diffusion kinetics of this antibody are highly heterogeneous. These spatially-dependent diffusivities were found to be related to local structure and composition ($0.3 < R^2 < 0.9$). When the collagen structure near the articular surface of samples was disrupted with collagenase, correlations increased in strength ($R^2 > 0.75$) and these samples exhibited much higher (up to an order of magnitude) local diffusivities at the surface. Ultimately, this study reveals that the aligned collagen at the articular surface of healthy cartilage dominates diffusive hindrance of large therapeutics.

This study used two enzymes (trypsin and collagenase) to target proteoglycans and collagen. In cartilage, trypsin cleaves the aggrecan core protein, releasing sulfated GAG chains from aggrecan (and other smaller proteoglycans) (Bonassar et al., 1995; Torzilli et al., 1997; Xia et al., 1995) from the tissue. In addition to removing proteoglycans (Billinghurst, 1997; Fosang et al., 1996), collagenase denatures the triple helix of collagen II, cleaving the collagen molecule into smaller fragments and degrading intermolecular crosslinks that enable formation of organized fibrils (Billinghurst, 1997). Use of FTIR showed that collagenase and trypsin both decrease local concentrations of proteoglycans. Unexpectedly, FTIR did not demonstrate differences for absolute collagen concentrations between healthy and collagenase-treated groups (Supplementary Fig. 2). However, use of SHG images revealed lower amounts of organized collagen at the surface of collagenase-treated samples within the first 50 μm. Thus, collagenase did not have enough time to remove significant amounts of collagen protein from the matrix, but was able to disrupt collagen organization by fragmenting collagen fibrils (Billinghurst, 1997). This study therefore elucidates how macromolecular transport is affected by changes in collagen structure and depletion of aggrecan.

Making local measurements revealed that enzymatic treatment had the most profound effect on the diffusivity of the surface region. Application of trypsin or collagenase resulted in higher local diffusivities (up to 10-fold compared to healthy) at depths up to 400 μm from the tissue surface. Although both trypsin and collagenase treatments increased sample diffusivities, collagenase-treated samples exhibited significantly higher diffusivities than trypsin treated within 0–100 μm of the surface (Fig. 2). Because both enzymes removed similar amounts of proteoglycans in this region, the higher local diffusivities in collagenase-treated samples are likely due to disruption of the highly aligned collagen at the surface.

Correlations between local composition and diffusivity also point to the importance of organized collagen in the surface layer on macromolecular transport. Across all depths, healthy samples had the weakest correlations between composition and local diffusivity ($R^2 < 0.46$), whereas these correlations for collagenase-treated samples were stronger ($R^2 > 0.75$). In general, correlations were weakened in healthy samples by regions in the top 100 μm (light points in Fig. 5), which had much lower diffusivity than would be predicted by relationships formed from the middle and deep regions of samples (dark points in Fig. 5). Removal of aggrecan by trypsin improved this aggrecan/diffusivity correlation only slightly, with the surface region clearly having lower diffusivity than expected. In contrast, disruption of surface collagen by collagenase dramatically increased surface diffusivity (up to 10-fold compared to healthy), resulting in a single linear correlation (for both aggrecan and collagen content) that described all regions of

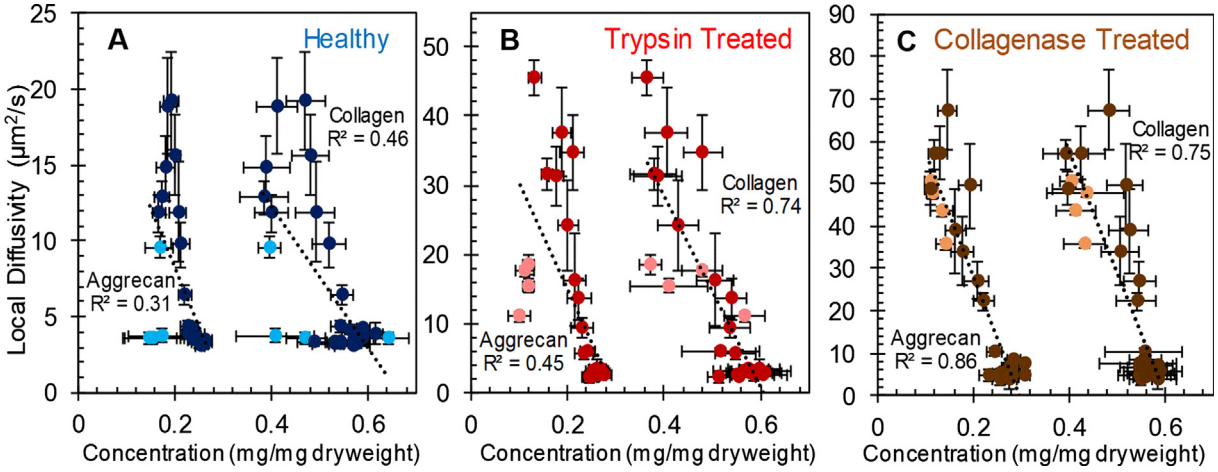

Fig. 5. Correlations comparing local diffusivities from the transport analysis to the local composition obtained from FTIR and SHG for healthy (A), trypsin-treated (B), and collagenase-treated (C) groups. Lighter shaded data designate points near the articular surface of samples (within 0–100 μm). Overall, concentrations of collagen and aggrecan were negatively correlated with local diffusivity in all groups. The slopes of the diffusivity/composition correlations for local aggrecan and collagen content are −78 and −47 for healthy samples, −153 and −138 for trypsin-treated samples, and −293 and −285 for collagenase-treated samples, respectively. Aggrecan and collagen content were more strongly correlated with diffusivity in the degraded groups (trypsin: $R^2 = 0.45$, 0.74, $p < 0.001$; collagenase: $R^2 = 0.86$, 0.75, $p < 0.001$), compared to the healthy group ($R^2 = 0.31$, 0.46, $p < 0.01$). Additionally, aggrecan and collagen correlations for collagenase-treated samples exhibited steeper diffusivity/concentration relationships compared to correlations from the healthy group ($p < 0.05$, ANCOVA).

the tissue (Supplementary Fig. 3). Because the only major change between collagenase and trypsin treatment is collagen structure within this surface region (see Figs. 3 and 4), this further supports the conclusions that an intact collagenous surface zone acts as a selective barrier to large solutes and that aggrecan content is a strong predictor of diffusivity in degraded cartilage and in the deeper zones of healthy cartilage.

Although the highly aligned collagen layer at the surface has major implications for macromolecular transport, there is strong evidence that aggrecan concentration is more important for transport deeper in the tissue, where collagen content was similar for all groups. Compared to healthy samples at 150 μm, aggrecan content was ~43% lower for collagenase-treated samples and 25% lower for trypsin-treated samples, whereas diffusivities were ~4 and 3 times higher in this region, respectively. Thus, even a small decrease in aggrecan content can lead to a significant increase in local diffusivity for large solutes. These data are consistent with data from smaller molecules in mature bovine tissue (5 kDa inulin and 70 kDa dextran) (Torzilli et al., 1997). Similarly, decreases in aggrecan content have increased bulk diffusivities of a variety of solutes (with greater relative diffusivity changes for larger solutes) in both healthy and diseased human cartilage (Maroudas, 1970). Ultimately, both the surface layer and aggrecan content are critical factors in determining macromolecular transport throughout the depth of cartilage.

While this study uses a well-established and validated experimental procedure for antibody diffusion (DiDomenico et al., 2017, 2016), using these degradative enzymes raises some unanswered questions. Although desired, it is currently unknown how to degrade only the collagen matrix without affecting aggrecan in cartilage. As such, the correlations obtained for collagenase-treated samples intrinsically include effects from degrading both constituents of cartilage. However, this type of degradation is more likely clinically relevant, since natural degradation *in vivo* would be similar to collagenase degradation (Billinghurst, 1997). There is also reason to believe that the local partition coefficient is being significantly affected by degradation of the aggrecan in the tissue. Fluorescence images show large bands of increased fluorescence that match up well with areas of lower aggrecan content from histology (Fig. 2). Thus, it is likely that these areas are experiencing higher local partition coefficients, but these were not calculated in this study. These experiments were not conducted on mature cartilage tissue, but the structure and heterogeneities of articular cartilage are similar across species and age (Klein et al., 2007; Poole et al., 2001). Strong trends were found between diffusivity and solute size across many different types of cartilage, including adult human (DiDomenico et al., 2018). Thus, the composition and diffusivity relationships are likely transferrable to cartilage of various age and species. Finally, this study did not explicitly measure the role of collagen fiber diameter on local diffusion. Since another study found no lateral diffusional changes throughout the middle and deep zones (DiDomenico et al., 2016), collagen orientation and fiber size seem to be most important in areas of lower aggrecan content, such as the surface region. Furthermore, our data and previous data on antibody diffusion (DiDomenico et al., 2017) support that diffusion of larger solutes are hindered more so than smaller solutes in the surface zone.

With the application of FTIR and SHG techniques in combination with well-established diffusion protocols (DiDomenico et al., 2017, 2016), this is the first study to directly examine the relationship between local structure/composition and local diffusion mechanics of a large therapeutic antibody (150 kDa) in cartilage. Overall, the local diffusivity was well predicted by both local concentrations of aggrecan and collagen, and the highly aligned collagen at the articular surface was found to dramatically hinder transport of antibodies into the tissue. These relationships are relevant to both healthy and diseased human cartilage and can be used to help inform and develop targeted therapies based on local composition and collagen orientation.

Acknowledgments

This work was supported by the National Science Foundation grant (NSF-1536463). This work made use of the Cornell Center for Materials Research Shared Facilities which are supported through the NSF MRSEC program (DMR-1719875). This work made use of imaging equipment under grants: NIH S10RR025502, NYSTEM CO29155, and NIH S10OD018516.

Conflict of interest statement

Material support was in part provided by AbbVie Inc.

Appendix A. Supplementary material

Supplementary data to this article can be found online at https://doi.org/10.1016/j.jbiomech.2018.10.019.

References

Allen, K.D., Adams, S.B., Setton, L.A., 2010. Evaluating intra-articular drug delivery for the treatment of osteoarthritis in a rat model. Tissue Eng. Part B. Rev. 16, 81–92. https://doi.org/10.1089/ten.teb.2009.0447.

Ballyns, J.J., Gleghorn, J.P., Niebrzydowski, V., Rawlinson, J.J., Potter, H.G., Maher, S. A., Wright, T.M., Bonassar, L.J., 2008. Image-guided tissue engineering of anatomically shaped implants via MRI and micro-CT using injection molding. Tissue Eng. Part A 14, 1195–1202. https://doi.org/10.1089/ten.tea.2007.0186.

Bank, R.A., Krikken, M., Beekman, B., Stoop, R., Maroudas, A., Lafebers, F.P.J.G., Te Koppele, J.M., 1997. A simplified measurement of degraded collagen in tissues: application in healthy, fibrillated and osteoarthritic cartilage. Matrix Biol. 16, 233–243. https://doi.org/10.1016/S0945-053X(97)90012-3.

Bank, R.A., Soudry, M., Maroudas, A., Mizrahi, J., Tekoppele, J.M., 2000. The increased swelling and instantaneous deformation of osteoarthritic cartilage is highly correlated with collagen degradation. Arthritis Rheum. 43, 2202–2210. https://doi.org/10.1002/1529-0131(200010)43:10<2202::AID-ANR7>3.0.CO;2-E.

Billinghurst, R.C., 1997. Enhanced cleavage of type II collagen by collagenase in osteoarthritic articular cartilage. J. Clin. Invest 99, 1534–1545. https://doi.org/10.1172/JCI119316.

Bonassar, L.J., Frank, E.H., Murray, J.C., Paguio, C.G., Moore, V.L., Lark, M.W., Sandy, J. D., Wu, J.J., Eyre, D.R., Grodzinsky, A.J., 1995. Changes in cartilage composition and physical properties due to stromelysin degradation. Arthritis Rheum. 38, 173–183. https://doi.org/10.1002/art.1780380205.

Camacho, N.P., West, P., Torzilli, P.A., Mendelsohn, R., 2001. FTIR microscopic imaging of collagen and proteoglycan in bovine cartilage. Biopolym. – Biospectrosc. Sect. 62, 1–8. https://doi.org/10.1002/1097-0282(2001) 62:1<1::AID-BIP10>3.0.CO;2-O.

Carr, E.J., Turner, I.W., 2015. A semi-analytical solution for multilayer diffusion in a composite medium consisting of a large number of layers. Appl. Math. Model. 40, 7034–7050. https://doi.org/10.1016/j.apm.2016.02.041.

Case, J.P., Sano, H., Lafyatis, R., Remmers, E.F., Kumkumian, G.K., Wilder, R.L., 1989. Transin/stromelysin expression in the synovium of rats with experimental erosive arthritis. In situ localization and kinetics of expression of the transformation-associated metalloproteinase in euthymic and athymic Lewis rats. J. Clin. Invest. 84, 1731–1740. https://doi.org/10.1172/JCI114356.

Chan, C.E.Z., Chan, A.H.Y., Hanson, B.J., Ooi, E.E., 2009. The use of antibodies in the treatment of infectious diseases. Singapore Med. J. 50, 663–672. quiz 673.

Chen, X., Nadiarynkh, O., Plotnikov, S., Campagnola, P.J., 2012. Second harmonic generation microscopy for quantitative analysis of collagen fibrillar structure. Nat. Protoc. 7, 654–669. https://doi.org/10.1038/nprot.2012.009.

Chin, J.R., Murphy, G., Werb, Z., 1985. Stromelysin, a connective tissue-degrading metalloendopeptidase secreted by stimulated rabbit synovial fibroblasts in parallel with collagenase: biosynthesis, isolation, characterization, and substrates. J. Biol. Chem. 260, 12367–12376.

Clark, R.A., 2001. A critical comparison of two long-term zooplankton time series from the central-west North Sea. J. Plankton Res. 23, 27–39. https://doi.org/10.1093/plankt/23.1.27.

DiDomenico, C.D., Lintz, M., Bonassar, L.J., 2018. Molecular transport in articular cartilage – what have we learned from the past 50 years? Nat. Rev. Rheumatol. 14 (7), 393–403.

DiDomenico, C.D., Goodearl, A., Yarilina, A., Sun, V., Mitra, S., Sterman, A.S., Bonassar, L.J., 2017. The effect of antibody size and mechanical loading on solute diffusion through the articular surface of cartilage. J. Biomech. Eng. 139,. https://doi.org/10.1115/1.4037202 091005.

DiDomenico, C.D., Xiang Wang, Z., Bonassar, L.J., 2016. Cyclic mechanical loading enhances transport of antibodies into articular cartilage. J. Biomech. Eng. 139,. https://doi.org/10.1115/1.4035265 011012.
Elliott, D.M., Narmoneva, D.A., Setton, L.A., 2002. Direct measurement of the poisson's ratio of human patella cartilage in tension. J. Biomech. Eng. 124, 223–228. https://doi.org/10.1115/1.1449905.
Enobakhare, B.O., Bader, D.L., Lee, D.a., 1996. Quantification of sulfated glycosaminoglycans in chondrocyte/alginate cultures, by use of 1,9-dimethylmethylene blue. Anal. Biochem. 243, 189–191. https://doi.org/10.1006/abio.1996.0502.
Evans, C.H., Kraus, V.B., Setton, L.A., 2013. Progress in intra-articular therapy. Nat. Rev. Rheumatol. 10, 11–22. https://doi.org/10.1038/nrrheum.2013.159.
Feldmann, M., Maini, R.N., 2001. Anti -TNFα therapy of rheumatoid arthritis: what have we learned? Annu. Rev. Immunol. 19, 163–196.
Fosang, A.J., Last, K., Knäuper, V., Murphy, G., Neame, P.J., 1996. Degradation of cartilage aggrecan by collagenase-3 (MMP-13). FEBS Lett. 380, 17–20. https://doi.org/10.1016/0014-5793(95)01539-6.
Gerwin, N., Hops, C., Lucke, A., 2006. Intraarticular drug delivery in osteoarthritis. Adv. Drug Deliv. Rev. 58, 226–242. https://doi.org/10.1016/j.addr.2006.01.018.
Goldring, M.B., 2001. Anticytokine therapy for osteoarthritis. Exp. Opin. Biol. Ther. 1, 817–829. https://doi.org/10.1517/14712598.1.5.817.
Griffin, D.J., Vicari, J., Buckley, M.R., Silverberg, J.L., Cohen, I., Bonassar, L.J., 2014. Effects of enzymatic treatments on the depth-dependent viscoelastic shear properties of articular cartilage. J. Orthop. Res. 32, 1652–1657. https://doi.org/10.1002/jor.22713.
Hayes, W.C., Bodine, A.J., 1978. Flow-independent viscoelastic properties of articular cartilage matrix. J. Biomech. 11, 407–419. https://doi.org/10.1016/0021-9290(78)90075-1.
Hwang, W.S., Li, B., Jin, L.H., Ngo, K., Schachar, N.S., Hughes, G.N., 1992. Collagen fibril structure of normal, aging, and osteoarthritic cartilage. J. Pathol. 167, 425–433. https://doi.org/10.1002/path.1711670413.
Khanarian, N.T., Boushell, M.K., Spalazzi, J.P., Pleshko, N., Boskey, A.L., Lu, H.H., 2014. FTIR-I compositional mapping of the cartilage-to-bone interface as a function of tissue region and age. J. Bone Miner. Res. 29, 2643–2652. https://doi.org/10.1002/jbmr.2284.
Klein, T.J., Chaudhry, M., Bae, W.C., Sah, R.L., 2007. Depth-dependent biomechanical and biochemical properties of fetal, newborn, and tissue-engineered articular cartilage. J. Biomech. 40, 182–190. https://doi.org/10.1016/j.jbiomech.2005.11.002.
Leddy, H.A., Guilak, F., 2003. Site-specific molecular diffusion in articular cartilage measured using fluorescence recovery after photobleaching. Ann. Biomed. Eng. 31, 753–760. https://doi.org/10.1114/1.1581879.
Leddy, H.A., Haider, M.A., Guilak, F., 2006. Diffusional anisotropy in collagenous tissues: fluorescence imaging of continuous point photobleaching. Biophys. J. 91, 311–316. https://doi.org/10.1529/biophysj.105.075283.
Lotke, P.A., Granda, J.L., 1972. Alterations in the permeability of articular cartilage by proteolytic enzymes. Arthritis Rheum. 15, 302–308. https://doi.org/10.1002/art.1780150312.
MacNaul, K.L., Chartrain, N., Lark, M., Tocci, M.J., Hutchinson, N.I., 1990. Discoordinate expression of stromelysin, collagenase, and tissue inhibitor of metalloproteinases-1 in rheumatoid human synovial fibroblasts: synergistic effects of interleukin-1 and tumor necrosis factor-?? on stromelysin expression. J. Biol. Chem. 265, 17238–17245.
Maroudas, A., 1975. Biophysical chemistry of cartilaginous tissues with special reference to solute and fluid transport. Biorheology 12, 233–248.
Maroudas, A., 1970. Distribution and diffusion of solutes in articular cartilage. Biophys. J. 10, 365–379. https://doi.org/10.1016/S0006-3495(70)86307-X.
Maroudas, A., Bullough, P., 1968. Permeability of articular cartilage. Nature 219, 1260–1261. https://doi.org/10.1038/2191260a0.
Martel-Pelletier, J., 2004. Pathophysiology of osteoarthritis. Osteo. Cartil. 12 (Suppl A), S31–S33. https://doi.org/10.1053/joca.1998.0140.
Martel-Pelletier, J., McCollum, R., Fujimoto, N., Obata, K., Cloutier, J.M., Pelletier, J.P., 1994. Excess of metalloproteases over tissue inhibitor of metalloprotease may contribute to cartilage degradation in osteoarthritis and rheumatoid arthritis. Lab Invest 70, 807–815.
Middendorf, J.M., Shortkroff, S., Dugopolski, C., Kennedy, S., Siemiatkoski, J., Bartell, L.R., Cohen, I., Bonassar, L.J., 2017. In vitro culture increases mechanical stability of human tissue engineered cartilage constructs by prevention of microscale scaffold buckling. J. Biomech. 64, 77–84. https://doi.org/10.1016/j.jbiomech.2017.09.007.
Moos, V., Fickert, S., Müller, B., Weber, U., Sieper, J., 1999. Immunohistological analysis of cytokine expression in human osteoarthritic and healthy cartilage. J. Rheumatol. 26, 870–879.
Mow, V.C., Holmes, M.H., Michael Lai, W., 1984. Fluid transport and mechanical properties of articular cartilage: a review. J. Biomech. 17, 377–394. https://doi.org/10.1016/0021-9290(84)90031-9.
Neuman, R.E., Logan, M.A., 1950. The determination of hydroxyproline. J. Biol. Chem. 184, 299–306. https://doi.org/10.1016/0009-8981(65)90038-0.
Nguyen, Q., Murphy, G., Roughley, P.J., Mort, J.S., 1989. Degradation of proteoglycan aggregate by a cartilage metalloproteinase. Evidence for the involvement of stromelysin in the generation of link protein heterogeneity in situ. Biochem. J. 259, 61–67.
Pelletier, J.P., Martel-Pelletier, J., Malemud, C.J., 1988. Canine osteoarthritis: Effects of endogenous neutral metalloproteoglycanases on articular cartilage proteoglycans. J. Orthop. Res. 6, 379–388. https://doi.org/10.1002/jor.1100060309.
Poole, A.R., Kojima, T., Yasuda, T., Mwale, F., Kobayashi, M., Laverty, S., 2001. Composition and structure of articular cartilage: a template for tissue repair. Clin. Orthop. Relat. Res. 1, S26–S33 https://doi.org/11603710.
Saarakkala, S., Julkunen, P., 2010. Specificity of Fourier Transform Infrared (FTIR) microspectroscopy to estimate depth-wise proteoglycan content in normal and osteoarthritic human articular cartilage. Cartilage 1, 262–269. https://doi.org/10.1177/1947603510368689.
Shimizu, Y., Ohta, M., 2015. Influence of plaque stiffness on deformation and blood flow patterns in models of stenosis. Biorheology 52, 171–182. https://doi.org/10.3233/BIR-14016.
Silverberg, J.L., Barrett, A.R., Das, M., Petersen, P.B., Bonassar, L.J., Cohen, I., 2014. Structure-function relations and rigidity percolation in the shear properties of articular cartilage. Biophys. J. 107, 1721–1730. https://doi.org/10.1016/j.bpj.2014.08.011.
Sun, H.B., 2010. Mechanical loading, cartilage degradation, and arthritis. Ann. N.Y. Acad. Sci. 1211, 37–50. https://doi.org/10.1111/j.1749-6632.2010.05808.x.
Torzilli, P.A., Arduino, J.M., Gregory, J.D., Bansal, M., 1997. Effect of proteoglycan removal on solute mobility in articular cartilage. J. Biomech. 30, 895–902. https://doi.org/10.1016/S0021-9290(97)00059-6.
Treppo, S., Koepp, H., Quan, E.C., Cole, A.A., Kuettner, K.E., Grodzinsky, A.J., 2000. Comparison of biomechanical and biochemical properties of cartilage from human knee and ankle pairs. J. Orthop. Res. 18, 739–748. https://doi.org/10.1002/jor.1100180510.
Venn, M., Maroudas, A., 1977. Chemical composition and swelling of normal and osteoarthrotic femoral head cartilage. I. Chemical composition. Ann. Rheum. Dis. 36, 121–129. https://doi.org/10.1136/ard.36.2.121.
Williamson, A.K., Chen, A.C., Masuda, K., Thonar, E.J.M.A., Sah, R.L., 2003. Tensile mechanical properties of bovine articular cartilage: Variations with growth and relationships to collagen network components. J. Orthop. Res. 21, 872–880. https://doi.org/10.1016/S0736-0266(03)00030-5.
Wilson, W., Van Donkelaar, C.C., Van Rietbergen, B., Ito, K., Huiskes, R., 2004. Stresses in the local collagen network of articular cartilage: a poroviscoelastic fibril-reinforced finite element study. J. Biomech. 37, 357–366. https://doi.org/10.1016/S0021-9290(03)00267-7.
Xia, Y., Farquhar, T., Burton-Wurster, N., Vernier-Singer, M., Lust, G., Jelinski, L.W., 1995. Self-diffusion monitors degraded cartilage. Arch. Biochem. Biophys. 323, 323–328. https://doi.org/10.1006/ABBI.1995.9958.
Zhu, W., Mow, V.C., Koob, T.J., Eyre, D.R., 1993. Viscoelastic shear properties of articular cartilage and the effects of glycosidase treatments. J. Orthop. Res. 11, 771–781. https://doi.org/10.1002/jor.1100110602.